33rd Annual International Conference of the IEEE EMBS
Boston, Massachusetts USA, August 30 - September 3, 2011

Model-based Segmentation of Flexor Tendons from Magnetic Resonance Images of Finger Joints

H.C. Chen, C.K. Chen, T.H. Yang, L.C. Kuo, I.M. Jou, F.C. Su, and Y.N. Sun

***Abstract*—Trigger finger is a common hand disease, causing swelling, painful popping and clicking in moving the affected finger joint. To better evaluate patients with trigger finger, segmentation of flexor tendons from magnetic resonance (MR) images of finger joints, which can offer detailed structural information of tendons to clinicians, is essential. This paper presents a novel model-based method with three stages for automatically segmenting the flexor tendons. In the first stage, a set of tendon contour models (TCMs) is initialized from the most proximal cross-sectional image via two-step ellipse estimation. Each of the TCMs is then propagated to its distally adjacent image by affine registration. The propagation is sequentially performed along the proximal-distal direction until the most distal image is reached, as the second stage of segmentation. The TCMs on each cross-sectional image are refined in the last stage with the snake deformation. MR volumes of three subjects were used to validate the segmentation accuracy. Compared with the manual results, our method showed good accuracy with small average margins of errors (within 0.5 mm) and large overlapping ratio (dice similarity coefficient above 0.8). Overall, the proposed method has great potential for morphological change assessment of flexor tendons and pulley-tendon system modeling for image guided surgery.**

I. Introduction

THE human hand, which is capable of carrying out complex tasks, such as object grasping, is the epitome of an essential anatomical structure. Unfortunately, long-term activities or heavy loads may lead to irritation of the flexor tendons in finger joints. While the irritation becomes serious, nodule or thickening may be developed on the tendons, producing non-smoothness or even pain when the tendons pass through the pulleys. A trigger finger also known as stenosing tenosynovitis then occurs. Recently, the trigger finger has become a common hand problem. To provide better evaluation and diagnosis for patients with trigger finger, segmentation of the flexor tendons from magnetic resonance (MR) images of finger joints, which can offer detailed structural information (e.g., size of tendon) to clinicians, hence becomes an important issue.

As a finger joint is a quite small region, near which rigid (e.g., phalanges) and soft tissues (e.g., tendons, sheaths, pulleys and ligaments) are located, segmentation of the flexor tendons in finger joints from MR images usually suffers from susceptibility artifact and partial volume effect [1]. These artifacts lead to some difficulties in segmenting MR tendon images. For example, fuzzy boundaries between tendons and their surrounding tissues make it difficult to precisely capture the tendon boundaries. Moreover, several irrelevant tissues (e.g., ligament and vessel) with similar intensity to tendons' may perplex the automatic identification of tendon regions.

According to our trials, purely pixel classification-based and region-based methods [2][3], which consider intensity characteristics only, are insufficient for handling these difficulties. In contrast, deformable model-based methods usually incorporate the prior shape knowledge of a target object with image intensity information into the segmentation process. They are thus supposed to be ideal for MR tendon image segmentation. Kaus et al. [4] proposed using a deformable model-based method to automatically construct the point distribution model from a set of segmented volumetric images. Their method measured the degree of shape distortion from a reference mesh to constrain the model deformation, and thus achieved the segmentation stably. Sotoca et al. [5] adopted the statistical shape model to constrain the segmentation process to handle the difficulty of fuzzy boundary in hand X-ray images. Yet, these methods require manual adjustment, which is tedious and operator dependent, to provide the model with a proper initial condition for avoiding being trapped in the local optima.

Automatic initialization for deformable model-based segmentation is often thought of as an application-dependent issue. Recently, Yu et al. [6] and Chen et al. [7] proposed using Hough transform and articulated registration for fetal head and hand bone segmentations respectively, to automatically obtain good initial models. Compared to the tendons in finger joints, there is quite large variability in either shape of target tissues or geometric relationship between neighboring tissues, so the previously developed methods may not be applicable. To the best of our knowledge, the issue in automatic segmentation of the flexor tendons in finger joints has not been well addressed in other research yet.

In this paper we propose a novel model-based method for automatically segmenting the flexor tendons from the MR images of finger joints. The proposed method consists of major features as follows. First, we design a two-step ellipse estimation approach to achieve automatic initialization of tendon contour models (TCMs). Second, we present a

Manuscript received March 26, 2011. Y.N. Sun, H.C. Chen and C.K. Chen are with Department of Computer Science and Information Engineering, National Cheng Kung University, Tainan, Taiwan, R.O.C.; T.H. Yang and F.C. Su are with Institute of Biomedical Engineering, National Cheng Kung University, Tainan, Taiwan, R.O.C.; L.C. Kuo is with Department of Occupational Therapy, National Cheng Kung University, Taiwan, R.O.C.; I.M. Jou is with Department of Orthopedics, National Cheng Kung University Hospital, Tainan, Taiwan, R.O.C..

Corresponding author: Y.N. Sun; phone: +886 -2757575-62526; fax: +886-2747076; e-mail: ynsun@mail.ncku.edu.tw.

contour model propagation strategy, which effectively compensates the changes in position, orientation and scale of flexor tendons between adjacent cross-sectional images, to provide the subsequent snake deformation with a good initial condition. Third, prior shape knowledge of tendon structures is incorporated in the segmentation process for avoiding excessive tendon shape distortion. Overall, the proposed method can overcome the aforementioned difficulties in segmenting MR tendon images, thus achieving promising segmentation results.

II. Initialization of Tendon Contour Models

A. Region of Interest Identification in MR Axial Image

We can observe from MR axial images of finger joints that the flexor and extensor tendons are very similar in shape and intensity (see Fig. 1a). Identifying a region of interest (ROI), which includes the flexor tendons and excludes the extensor tendons, is supposed to be a helpful step for avoiding confusion in the subsequent segmentation process. From an anatomical point of view, the flexor and extensor tendons are located at the palmar and dorsal sides of the hand, respectively. Such anatomical knowledge is used to obtain the desirable ROI.

At first, some fundamental image processing techniques including thresholding, morphological closing operator and connected component searching are adopted to extract the hand region (indicated by the white region in Fig. 1b) from the most proximal cross-sectional image. Then, the ROI for flexor tendon segmentation is specified by the region enclosed by the blue curve in Fig. 1b. The distances, from the left border of the ROI to the left margin of the image, and from the right border of the ROI to the right margin of the image, are set to one-eighth of the image width. The bottom border of the ROI is represented by the palmar-side boundary of the hand region, and the top border is obtained by shifting the bottom border with one-fifth of the image height toward the dorsal side of the hand.

B. Two-step Ellipse Estimation

Since the tendons in MR axial images are usually elliptic in shape, an ellipse is ideal for approximating their shape and position. In the proposed system, four tendon contour models (TCMs) are utilized to segment the tendons in four finger joints. Each TCM is initialized by estimating an ellipse, which is close to the flexor tendon on the most proximal image as much as possible. The pose of an ellipse is specified by several parameters, including lengths of major and minor axes, X- and Y-coordinates of center, and a tilt angle. We present a two-step ellipse estimation approach below based on the low-intensity property of tendons on MR images.

The two-step ellipse estimation approach first find the parameters of each TCM with respect to the horizontal direction, and then apply them as a spatial constraint to derive the other parameters on the vertical direction. In the first step, we count the pixels with intensities less than twenty-five

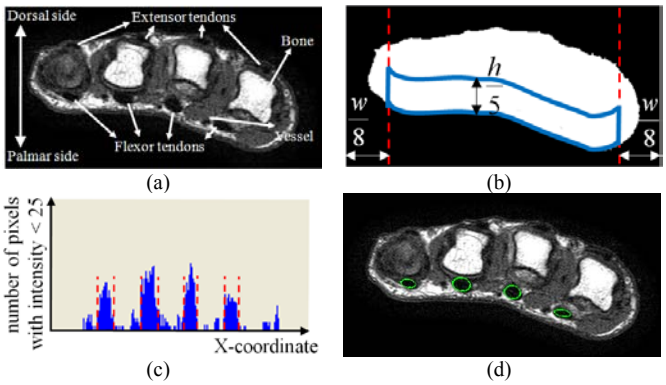

Fig. 1. Initialization of tendon contour models; (a) original MR axial image; (b) ROI of flexor tendons; (c) counting result in the first step of ellipse estimation; (d) initialized TCMs.

along each vertical line in the ROI. Fig. 1c shows the counting result, wherein the horizontal and vertical axes indicate the X-coordinate of the image and its corresponding number of counted pixels, respectively. It can be observed that the clusters bounded by the red dashed lines match to the flexor tendons, while the other smaller-sized clusters correspond to the vessels. In our experiments, the criterion to determine whether a cluster represents a tendon or not is that, its minimal height has to be larger than three pixels and its width has to be larger than fifteen pixels. We then calculate the distance between the margins of each cluster as the length of major axis of a TCM. Moreover, the X-coordinate of center of the TCM can be obtained by the average position of the corresponding margins.

In the second step of estimation, a similar counting process is performed, which is however along each horizontal line within four sub-regions of the ROI constrained by the TCMs' left and right ends. Thus, we can yield four counting results, from each of which the length of minor axis and the Y-coordinate of center of a TCM can be calculated. At last, we observe that the tilt angles of all TCMs are similar to the pronation/supination angle of the hand. They are hence assigned with the included angle between the horizontal axis and the vector, defined by connecting the centers of the TCMs in the index and little fingers respectively. The ellipse estimation result is demonstrated in Fig. 1d, wherein the position and shape of each TCM are close to those of the corresponding flexor tendon. In the rest of the paper, the points of the i-th TCM and its enclosed pixels are denoted as $\mathbf{M}_{k,i}$ and $\mathbf{R}_{k,i}$ respectively, where k is the index of cross-sectional images along the distal-proximal direction.

III. Contour Model Propagation

In general, there are certain positional offsets and size changes of flexor tendons between two adjacent cross-sectional images. The above ellipse estimation approach unfortunately may yield incorrect results in other cross-sectional images because of interference from some irrelevant tissues nearby the tendons and with low intensity as well. We hence present a contour model propagation strategy with affine registration to compensate such a spatial difference.

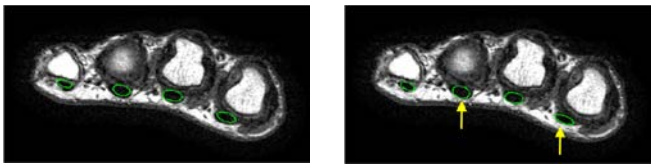

(a) (b)

Fig. 2. Contour model propagation; (a) before (b) after the affine registration.

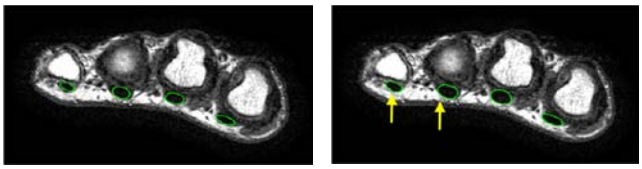

(a) (b)

Fig. 3. Model shape refinement; (a) before (b) after the snake deformation.

The propagation process begins with the most proximally cross-sectional image, is performed sequentially on each pair of adjacent cross-sectional images along the proximal-distal direction, and finally stops at the most distal image.

The registration is performed for each TCM by solving an affine transformation $\mathbf{T}_i$ which minimizes the cost function C_{reg}:

$$C_{reg} = \eta E_{intensity} + (1-\eta) E_{contrast} \quad (1)$$

$$E_{intensity} = \frac{1}{r_i} \sum_{a=1}^{r_i} I_{k-1}(\mathbf{T}_i \mathbf{R}_{k,i}(a)),$$

$$E_{contrast} = \frac{1}{2m_{k,i}} \sum_{j=1}^{m_{k,i}} \left(\sum_{a=1}^{2} I_{k-1}(\mathbf{T}_i \mathbf{M}_{k,i}(j) + a\mathbf{n}(\mathbf{T}_i \mathbf{M}_{k,i}(j))) - \sum_{a=-2}^{-1} I_{k-1}(\mathbf{T}_i \mathbf{M}_{k,i}(j) + a\mathbf{n}(\mathbf{T}_i \mathbf{M}_{k,i}(j))) \right),$$

where $E_{intensity}$ is the intensity energy representing the average intensity inside the registered tendon, and $E_{contrast}$ is the contrast energy indicating the average intensity difference between inside and outside regions of the TCM. $I_{k\text{-}1}$ is the (k-1)-th cross-sectional MR image. $m_{k,i}$ is the number of $\mathbf{M}_{k,i}$,and $\mathbf{n}(\mathbf{M}_{k,i}(j))$ represents the inward-pointing normal of the j-th point of the TCM. η is a weighting factor, and r_i is the number of $\mathbf{R}_{k,i}$.

Fig. 2 shows the tendon contours before and after the affine registration. After the contour propagation step, each registered TCM is closer to its corresponding position in the distally adjacent image, as indicated by the arrows. In the implementation the value of η was assigned with 0.5, and (1) was minimized using the Powell's multidimensional direction set method [8].

IV. Model Shape Refinement

In addition, there are certain local shape deviations between the registered TCMs and the true tendon boundaries on each cross-sectional image. Therefore, we design an algorithm of snake deformation to refine the shape of each TCM. The snake is deformed via minimizing the following energy E:

$$E(\mathbf{M}_{k,i}) = \sum_{j=1}^{m_{k,i}} \left(\alpha E_{edge} + \beta E_{region} + (1-\alpha-\beta) E_{shape} \right), \quad (4)$$

where E_{edge} is the edge energy, E_{region} is the region energy, and E_{shape} is the shape energy. α and β are weighting factors determining the trade-off between these energies.

The edge energy, which is used to capture the true tendon boundary at the transition from dark to bright (i.e., from inside tendon region toward outside), is given as

$$E_{edge} = I_k(\mathbf{M}_{k,i}(j) + \mathbf{n}(\mathbf{M}_{k,i}(j))) - I_k(\mathbf{M}_{k,i}(j) - \mathbf{n}(\mathbf{M}_{k,i}(j))). \quad (5)$$

Next, the region energy that maintains low intensity inside the deformable model is formulated as

$$E_{region} = \sum_{a=1}^{3} I_k(\mathbf{M}_{k,i}(j) + a\mathbf{n}(\mathbf{M}_{k,i}(j)). \quad (6)$$

The shape energy which keeps the deformable model elliptic in shape as much as possible is designed as

$$E_{shape} = \left| \cos^{-1}\left(\frac{\mathbf{c}_j \cdot \mathbf{c}_{j+1}}{\|\mathbf{c}_j\| \|\mathbf{c}_{j+1}\|} \right) - \cos^{-1}\left(\frac{\tilde{\mathbf{c}}_j \cdot \tilde{\mathbf{c}}_{j+1}}{\|\tilde{\mathbf{c}}_j\| \|\tilde{\mathbf{c}}_{j+1}\|} \right) \right|, \quad (7)$$

where $\mathbf{c}_j$ and $\mathbf{c}_{j+1}$ are ($\mathbf{M}_{k,i}(j\text{-}1)$-$\mathbf{M}_{k,i}(j)$) and ($\mathbf{M}_{k,i}(j\text{+}1)$-$\mathbf{M}_{k,i}(j)$), respectively. The two arccosine functions in (7) indicate the local shape curvature at the j-th point of deformable model and original reference model, respectively.

In our implementation, (4) was minimized by iteratively adjusting the positions of points on the TCM to fit the true tendon boundary along the normal directions of contour points. The values of α and β were set to 0.5 and 0.3, respectively. Fig. 3 shows the result of snake deformation. Compared to the tendon contours obtained by registration only, the refined TCMs better fit the true tendon boundaries as indicated by the arrows. After the TCMs on each image are refined, a stack of segmented cross-sectional images can be obtained as the final segmentation result of flexor tendons.

V. Experimental Results

The following experiments for validating the accuracy of the proposed method contained visual evaluation and quantitative analysis. In the experiments, MRI examination for three healthy subjects was performed using the same 1.5-T whole-body MR imaging system (Achieva; Philips Medical Systems, Best, the Netherlands). The obtained MR volumes with 16, 14, 13 cross-sections respectively were then included in the validation work. The same values of the system parameters including the weighting factors in (1) and (4) were utilized throughout the entire experiments.

Fig. 4 shows the segmentation results of the flexor tendons, in which the segmented contours were superimposed onto the MR images. Overall, our proposed method achieved satisfactory tendon segmentations with good fit and realistic shape, even in the presence of fuzzy boundaries and irrelevant tissues with similar intensity to tendons' (pointed by the solid and dashed arrows, respectively).

In the quantitative analysis, the automatic results were compared to the manual results of an expert that serve as the ground truth. The comparison was based on two distance

measures which are mean error (ME) and root mean square error (RMSE), and a spatial overlap index called dice similarity coefficient (DSC) [7]:

$$\mathrm{ME} = \sum_{d=1}^{N} \sqrt{(\boldsymbol{a}_d - \boldsymbol{g}_e)^2} \Big/ N, \tag{8}$$

$$\mathrm{RMSE} = \sqrt{\sum_{d=1}^{N} (\boldsymbol{a}_d - \boldsymbol{g}_e)^2 \Big/ N}, \tag{9}$$

$$\mathrm{DSC} = \frac{2|\mathbf{A} \cap \mathbf{G}|}{|\mathbf{A}| + |\mathbf{G}|}, \tag{10}$$

where $\boldsymbol{a}_d$ is the d-th contour point of the automatic result, and $\boldsymbol{g}_e$ is the e-th contour point of the ground truth that is the closest to $\boldsymbol{a}_d$, and N is the number of contour points of the automatic result. **A** and **G** are the pixels of flexor tendons in the automatic result and the ground truth, respectively. Generally, small values of ME and RMSE, and a large value of DSC indicate that the automatic results are consistent with the ground truth.

Table I lists the evaluation result. For each subject, the average values of ME and RMSE of all the cross-sectional images were less than 0.5 millimeter (mm). Compared with the maximal diameter (about 8.5 mm) of the flexor tendons among the axially cross-sectional images, the segmentation errors in ME and RMSE were considered as quite small. Moreover, the average values of DSC were all larger than 0.8, which is a threshold for a good overlap between two segmented regions. Consequently, the accuracy of the proposed method can be confirmed in some sense.

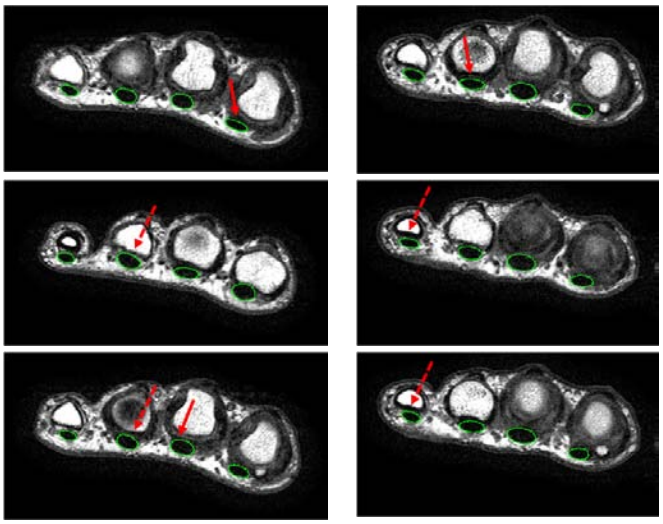

Fig. 4. Segmentation results of flexor tendons.

TABLE I. ACCURACY EVALUATION RESULT WITH ME, RMSE AND DSC IN (MEAN, STANDARD DEVIATION).

Subject	Average ME (mm)	Average RMSE (mm)	Average DSC (%)
1 (16)	(0.28, 0.05)	(0.43, 0.07)	(87.20, 1.56)
2 (14)	(0.29, 0.07)	(0.43, 0.11)	(86.94, 2.59)
3 (13)	(0.23, 0.10)	(0.35, 0.14)	(90.18, 4.15)
Average	(0.27, 0.07)	(0.40, 0.11)	(88.11, 2.77)

(.) represents the number of cross-sectional images.

VI. CONCLUSION

We have proposed a novel model-based segmentation method for the flexor tendons from the MR images of finger joints. A two-step ellipse estimation approach was first designed to automatically initialize a set of TCMs on the most proximal cross-sectional image. Then, we registered the TCMs to the remaining cross-sectional images via the contour model propagation strategy. Finally, prior shape knowledge of tendon structures that the tendons are nearly elliptic-shaped in axial-view images was incorporated into the snake algorithm for refining the shape of each TCM. Overall, our method utilized the structural constraint of the TCMs throughout the segmentation process, so reliable and accurate tendon segmentation can be achieved as demonstrated in the experimental results. In the future, the proposed method can be extended to segment the tendons of the whole hand for pulley-tendon system modeling. Also, this method can be used to measure geometric parameters of tendons (e.g., size) for evaluating the structural changes caused by trigger finger.

ACKNOWLEDGMENT

The authors would like to express their appreciation for the grant under contract NSC 99-2627-B-006-010 from the National Science Council, Taiwan (R.O.C.). Also, this work made use of shared facilities supported by the Program of Top 100 Universities Advancement, Ministry of Education, Taiwan (R.O.C.).

REFERENCES

[1] R.H. Hashemi, W.G. Bradley, and C.J. Lisanti, *MRI The Basics*, 2nd ed. Philadelphia, PA: Lippincott Williams & Wilkins, 2004.

[2] N. Otsu, "A threshold selection method from gray-Level histograms," *IEEE Trans. Sys., Man., Cyber.*, vol. 9, pp. 62–66, 1979.

[3] M. Sonka, V. Hlavac and R. Boyle, *Image Processing, Analysis, and Machine Vision*, 3rd ed. Toronto: Thomson Learning, 2007.

[4] M.R. Kaus, V. Pekar, C. Lorenz, R. Truyen, S. Lobregt, and J. Weese, "Automated 3-D PDM construction from segmented images using deformable models," *IEEE Trans. Med. Imag.*, vol. 22, pp. 1005–1013, 2003.

[5] J.M. Sotoca, J.M. Iñesta, and M.A. Belmonte, "Hand bone segmentation in radioabsorptiometry images for computerised bone mass assessment," *Comput. Med. Imaging Graphics*, vol. 27, pp. 459–467, 2003.

[6] J. Yu, Y. Wang, and P. Chen, "Fetal ultrasound image segmentation system and its use in fetal weight estimation," *Med. Bio. Eng. Comput.*, vol. 46: 1227–1237, 2008.

[7] H.C. Chen, I.M. Jou, C.K. Wang, F.C. Su, and Y.N. Sun, "Registration-based segmentation with articulated model from multipostural magnetic resonance images for hand bone motion animation," *Med. Phys.*, vol. 37, pp. 2670–2682, 2010.

[8] W.H. Press, S.A. Teukolsky, W.T. Vetterling, B.P. Flannery, *Numerical Recipes in C*, 2nd ed. Cambridge: Cambridge University Press, 1992.